Discovery of highly potent acid ceramidase inhibitors with tumor chemosensitizing activity

[1,2]Natalia Realini, [1]Carlos Solorzano, [2]Chiara Pagliuca, [2]Daniela Pizzirani,

[2]Andrea Armirotti, [3]Rosaria Luciani, [3]Maria Paola Costi, [2]Tiziano Bandiera, [1,2]Daniele Piomelli

[1]Department of Anatomy and Neurobiology, University of California, Irvine,

California 92697-4625

[2]Unit of Drug Discovery and Development, Italian Institute of Technology,

Genoa, Italy 16163

[3]Dipartimento di Scienze Farmaceutiche, University of Modena and Reggio Emilia,

Modena, Italy 41125

Supplementary Table S1

	vehicle	5-FU	0.1µM	0.3µM	1µM	3µM	10µM	30uM
d18:1/14:0	4.13±0.2	4.13±0.32	3.59±0.54	4.08±0.34	7.03±0.25	10.9±1.1***	16.9±0.37***	19.9±0.64***
d18:1/16:0	23.1±3.9	31.28±5.5	20.41±1	27.49±1.9	54.74±5.6*	105.7±3.2***	120.7±13.7***	142.1±12.2***
d18:1/18:0	0.26±0.1	0.15±0.05	0.58±0.06	0.40±0.02	0.72±0.23	0.49±0.09	1.001±0.19**	0.893±0.09*

Supplementary Table S1. Effects of carmofur or vehicle (DMSO, 0.1%) on ceramide levels in SW403 cells. Result are expressed in pmol-mg^{-1} protein as mean ± s.e.m. (n=4). *p<0.05 **p<0.01 ***p<0.001 vs vehicle, one-way ANOVA followed by Tukey's test.

Supplementary Table S2

	vehicle	5-FU	0.3µM	1µM	3µM
d18:1/14:0	1.49±0.09	1.48±0.09	1.44±0.06	1.59±0.12	1.99±0.11*
d18:1/16:0	99.79±7.88	116.71±6.72	114.76±6.96	145.44±9.58*	193.87±13.27***
d18:1/18:0	0.57±0.14	0.87±0.34	0.49±0.06	0.74±0.08	1.21±0.12

Supplementary Table S2. Effects of carmofur or vehicle (DMSO, 0.1%) on ceramide levels in LNCaP cells. Results are expressed in pmol-mg^{-1} protein as mean ± s.e.m. (n=4). *p<0.05 ***p<0.001 vs vehicle, one-way ANOVA followed by Tukey's test.

Supplementary Figure S1

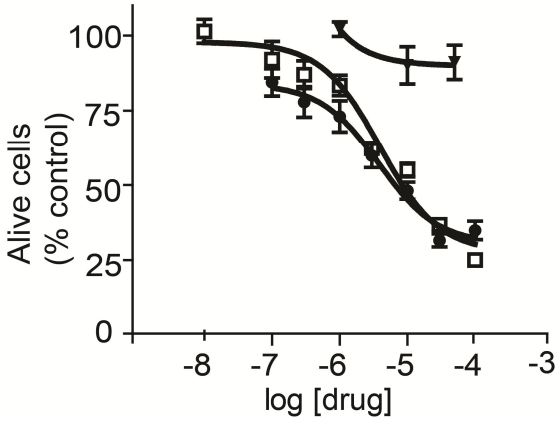

Supplementary Figure S1. Cytotoxic effects of carmofur and fumonisin B1 in Hek293 cells.

Concentration-response curve showing the effects of carmofur (□), fumonisin B1 (▾) or a combination of the two (●) on Hek293 cell viability, measured by Trypan blue assay. Results are expressed as mean ± s.e.m. (n=3).

Supplementary Figure S2

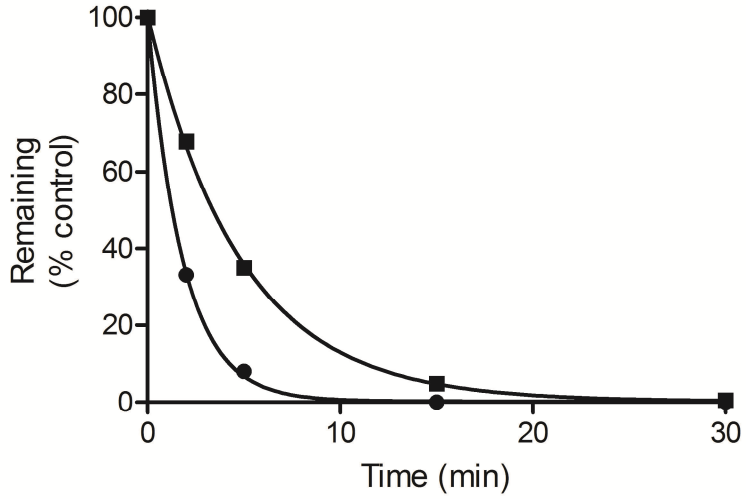

Supplementary Figure S2. Mouse plasma stability profiles of ARN080 and ARN398.

Half lives of ARN080 (■, 3.5min) and ARN398 (●, 1 min) were calculated using a one-phase decay fitting of LC-MS peak areas (n=3). Less than 5% variability was observed between triplicate timepoints. Average values are reported in the plot.

Supplementary Figure S3

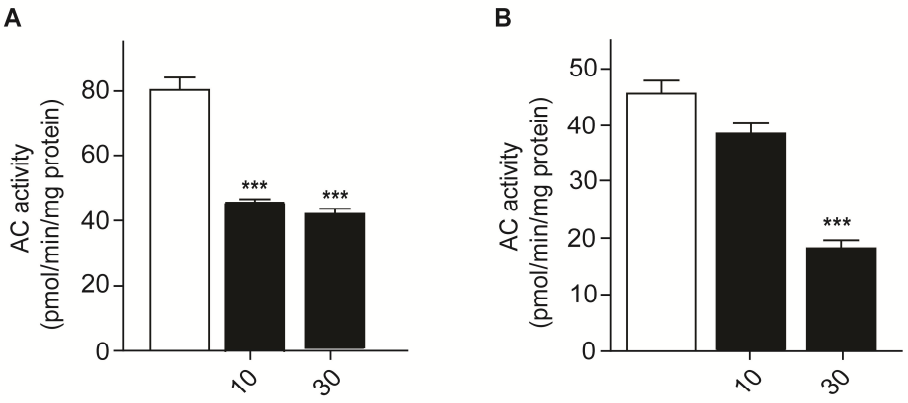

Supplementary Figure S3. ARN080 inhibits AC activity in live mice

Effects of ARN080 (closed bars) or vehicle (open bars) on AC activity in mouse (A) lung and (B) brain cortex. AC activity was measured ex vivo 2 h after injection of ARN080 (10 or 30 mg-kg^{-1}, i.p) or vehicle. Results are expressed as mean ± s.e.m. (n=6). *p<0.05, **p<0.01, ***p<0.001 vs vehicle, one-way ANOVA followed by Tukey's.

Supplementary Figure S4

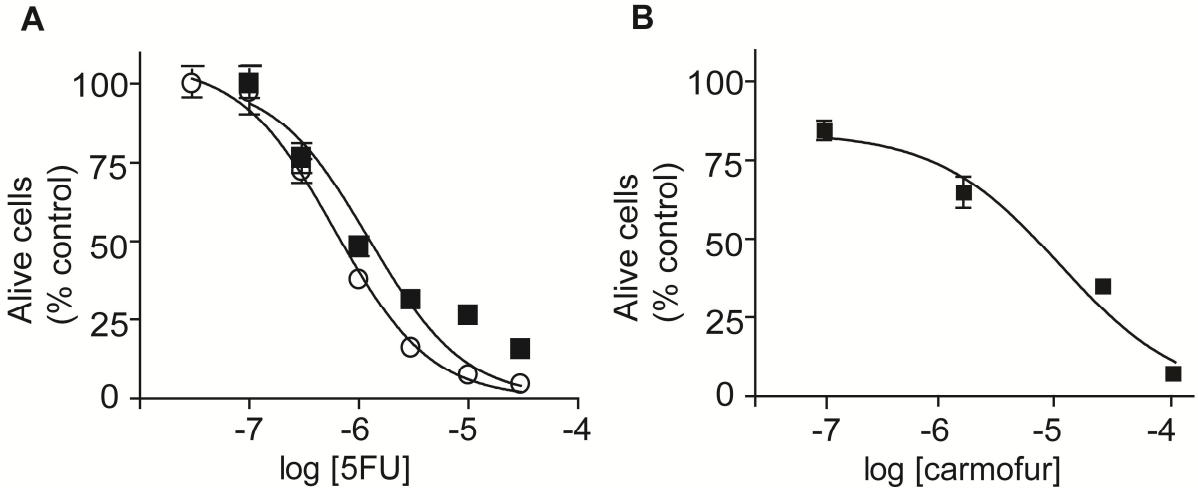

Supplementary Figure S4. Cytotoxic effects of carmofur and 5-FU in SW403 cells

(A) Concentration-response curve showing the effects of single (■) or multiple (○, 3 times in 72 h) exposure of SW403 cells to 5-FU. (B) Dose-response curve showing the effects of single exposure of SW403 cells to carmofur. Cell viability was evaluated using the Trypan blue assay. Results are expressed as mean ± s.e.m. (n=4).

Supplementary Figure S5

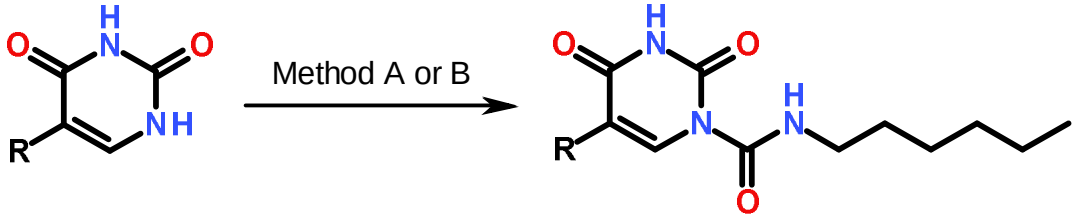

R = H, CH_3, Cl, CF_3

Supplementary Figure S5. Synthesis of N-hexyl-2,4-dioxo-pyrimidine 1-carboxamide derivatives. Method A: *n*-hexylisocyanate, DMSO, 50°c, 18h; Method B: *n*-hexylisocyanate, 4-dimethylaminopyridine, pyridine, r.t., 20h.

Supplementary Material and Methods

Acid Ceramidase Activity

Acid ceramidase activity was analyzed as previously described [1]. Briefly, cells or tissues were suspended in 20 mM Tris HCl (pH 7.5) containing 0.32M sucrose, sonicated and centrifuged at 800x*g* for 15 min at 4°C. The supernatants were centrifuged again at 12,000x*g* for 30 min at 4°C. The pellets were suspended in phosphate-buffered saline (PBS) and subjected to 2 freeze–thaw cycles at -80°C. The suspensions were centrifuged at 105,000x*g* for 1 h at 4 °C. The supernatants containing AC were kept at -80°C until use. Protein concentration was measured using the bicinchoninic acid (BCA) assay (Pierce).

AC activity was determined by incubating recombinant rat-AC (25 µg), cellular total lysate or protein fractionated from tissues (50 µg) in the presence of 100 µM *N*-lauroyl ceramide (Nu-Chek Prep, Elysian, MN) in assay buffer (100 mM sodium phosphate, 0.1% Nonidet P-40, 150 mM NaCl , 3 mM DTT, 100 mM sodium citrate, pH 4.5) for 30 min at 37 °C. Reactions were stopped by addition of a mixture of chloroform/methanol (2:1, vol/vol) containing 1 nmol heptadecanoic acid (HDA; NuChek Prep). The organic phases were collected, dried under nitrogen, and analyzed by LC/MS in the negative-ion mode monitoring the reaction product (lauric acid, m/z=199) using HDA as internal standard. Lipids were eluted on an XDB Eclipse C18 column isocratically at 2.2 mL-min^{-1} for 1 min with a solvent mixture of 95% methanol and 5% water, both containing 0.25% acetic acid and 5 mM ammonium acetate. The column temperature was 50°C. Electrospray ionization (ESI) was in the negative mode, capillary voltage was 4 kV, and fragmentor voltage was 100 V. Nitrogen was used as drying gas at a flow rate of 13 L- min^{-1} and at a temperature of 350°C. Nebulizer pressure was set at 60 psi. We monitored $[M-H]^-$ in the selected-ion monitoring (SIM). Calibration curves were generated with authentic lauric acid (Nu Check Prep).

Tissue Lipid Analyses

Lipid analysis was performed as previously described [2]. Lipids were extracted from mouse tissues with a chloroform/methanol mixture (2:1, vol/vol, 3 mL) containing internal standard [cer(d18:1/12:0)]. The organic phases were collected, dried under nitrogen and dissolved in methanol/chloroform (3:1, vol/vol) for LC/MS analyses. Ceramide species were identified and quantified by LC/MS^n, using a 1100-LC system (Agilent Technologies) equipped with an Ion Trap XCT and interfaced with electron spray ionization (ESI; Agilent Technologies). They were separated on a Poroshell 300 SB C18 column (2.1 x 75 mm i.d., 5 µm; Agilent Technologies) maintained at 30°C. A linear gradient of methanol in water containing 5 mM ammonium acetate and 0.25% acetic acid (from 80% to 100% of methanol in 3 min) was applied at a flow rate of 1 mL-min^{-1}. Detection was in the positive mode, capillary voltage was 4.5 kV, skimmer voltage -40V, and capillary exit -151V. Nitrogen was used as drying gas at a flow rate of 10 L-min^{-1}, temperature of 350°C, and nebulizer pressure of 80 psi. Helium was used as collision gas. Ceramide species were identified by comparison of their LC retention times and MS^n fragmentation patterns with those of authentic standards (Avanti Polar Lipids, Plymouth Meeting, PA). Extracted ion chromatograms were used to quantify cer(d18:1/14:0) (m/z 510.5 > 492.5 > 264.3), cer(d18:1/16:0) (*m*/*z* 538.5 > 520.3 > 264.3), cer(d18:1/18:0) (*m*/*z* 566.5 > 548.3 > 264.3), cer(d18:1/24:0) (*m*/*z* 650.5 > 632.3 > 264.3), cer(d18:1/24:1) (*m*/*z* 648.5 > 630.3 > 264.3) and using cer(d18:1/12:0) as internal standard (*m*/*z* 482.5 > 464.5 > 264.3). Detection and analysis were controlled using Agilent/Bruker Daltonics software version 5.2. MS spectra were processed using MS Processor from Advanced Chemistry Development.

Human Thymidylate synthetase purification and activity

Human Thymidylate synthetase purification and activity was performed as previously described[3,4]. Human Thymidylate Synthase (hTS) was cloned into a pQE80L system and recombinant protein was expressed in E. coli strain DH5α. Expression vector codes for a

hexahistidine tag at the N-terminus of the gene product designed to facilitate purification of the recombinant protein using immobilized metal affinity chromatography. Bacteria (DH5α/pQE80L) were cultured in 2 L of LB medium containing 100 µg ml^{-1} ampicilline at 37°c 120 rpm until the cultures attained at A_{600} of 0.6 and expression of hTS was induced with 1 mM isopropyl-b-D-thiogalactopyranoside (IPTG) for 4 hours at 37°c 120 rpm.

Cells were centrifuged at 4000 rpm for 30 min at 4°c. Cell pellet was suspended in 15 ml buffer A [NaH_2PO_4 (20 mM), NaCl (30 mM), pH 7,5)] containing protease inhibitors and sonicated six times for 10 s each at 4°c. Broken cells were centrifuged for 30 minutes at 12000 rpm at 4°C, supernatant was filtered at 0.80 µm and load in column Ni-HTP, prequilibrated with buffer A. Column was first washed with buffer A and then with buffer A + Imidazole (20 mM). Enzyme was eluted with buffer A containing 1 M imidazole. A fraction (1 mL) was loaded in HiTrap Desalting (GE Healthcare) column, preequilibrated with buffer buffer A and enzyme eluted with buffer A. Fractions (1 mL) containing the enzyme were collected in the hTS pool and stored at -80°c.

hTS activity was determined spectrophotometrically (Beckman DU640) by monitoring the increase in absorbance (340 nm) during the oxidation reaction of mTHF to DHF. The reaction mixture contained 50% TES buffer [(TES, N-[tris(hydroxymethyl)methyl]-2-aminoethanesulphonic acid (100 mM), $MgCl_2$ (50 mM), formalin (13 mM), EDTA (2 mM, pH 7.4), β-mercaptoethanol (150 mM)] , enzyme (0.1 µM), mTHF (50 µM), dUMP (120 µM) and water to 800 µl. The reaction was initiated when dUMP was added to the reaction mixture. Michaelis–Menten constant (K_M) was determined for mTHF and dUMP. Concentration ranges for the K_M measurements were 2–70 µM for mTHF and 2-100 µM for dUMP. Values for k_{cat} were also determined, hTS concentration ranges for measurements were 0,04–0,3 µM and mTHF (50 µM) and for dUMP (120 µM).

IC_{50} values were obtained by steady-state kinetic analysis at varying inhibitor concentration (0–100 µM) at two different time points (0 and 60 min). Analysis was carried out at room temperature in a mixture 50% of TES buffer, enzyme (0,09 µM), mTHF (45 µM), inhibitors and water to 600 µl. The reaction was started by adding dUMP (10µM) to the reaction mixture. IC_{50} values were obtained from the linear least-squares fit of the residual activity as function of inhibitor concentration, assuming classical binding competitive inhibition.

The results obtained are the mean ± standard deviation obtained in three independent experiments.

1 Solorzano, C. *et al.* Selective N-acylethanolamine-hydrolyzing acid amidase inhibition reveals a key role for endogenous palmitoylethanolamide in inflammation. *Proc. Natl. Acad. Sci. U S A* **106**, 20966-20971 (2009).

2 Snigdha, S. *et al.* Dietary and behavioral interventions protect against age related activation of caspase cascades in the canine brain. *PLoS One* **6,** e24652 (2011).

3 Cardinale, D., et al. Protein-protein interface-binding peptides inhibit the cancer therapy target human thymidylate synthase. *Proc. Natl. Acad. Sci. U S A*. **108**, E542-549 (2011).

4 Segel, I. H. Enzyme Kinetics. Behaviour and Analysis of Rapid Equilibrium and Steady-State Enzyme Systems; John Wiley and Sons: New York, p 105 (1993).